13 (2022) 100126

Contents lists available at ScienceDirect

International Journal of Thermofluids

journal homepage: www.sciencedirect.com/journal/international-journal-of-thermofluids

Modeling of thermal performance of a commercial alkaline electrolyzer supplied with various electrical currents

Tohid Adibi [a], Atta Sojoudi [b], Suvash C. Saha [c,*]

[a] School of Mechanical Engineering, University of Bonab, Bonab, Iran
[b] School of Mechanical Engineering College of Engineering. University of Tehran, Tehran, Iran
[c] School of Mechanical and Mechatronics Engineering, University of Technology Sydney, NSW 2007, Australia

ARTICLE INFO

Keywords:
Alkaline electrolyzer
Various electrical currents
Hydrogen production
Renewable energy
Thermal resistance

ABSTRACT

Hydrogen produced by solar and other clean energy sources is an essential alternative to fossil fuels. In this stuy, a commercial alkaline electrolyzer with different cell numbers and electrode areas are simulated for different pressure, temperature, thermal resistance, and electrical current. This alkaline electrolyzer is considered unsteady in simulations, and different parameters such as temperature are obtained in terms of time. The obtained results are compared with similar results in the literature, and good agreement is observed. Various characteristics of this alkaline electrolyzer as thermoneutral voltage, faraday efficiency and cell voltage are calculated and displayed. The outlet heat rate and generated heat rate are obtained as well. The pressure and the temperature in the simulations are between 1 and 100 bar and between 300 and 360 Kelvin respectively. The results show that the equilibrium temperature is reached 2–3 h after the time when the Alkaline electrolyzer starts to work.

1. Introduction

Environmental problems create a severe need for improved and cleaner energy sources. Companies and researchers are continuously working on this problem. There are two approaches for these research: either finding and proposing novel energy sources or enhancing the efficiency of current ones. Also, the new concerning issue for environmental maintenance has directed to lesser emissions of dangerous gasses. The common proposal emphasizes energy generated from renewable energy sources [1,2] and its following storing and carrying based on hydrogen [3,4]. Hydrogen is an eminent energy transporter due to its excellent energy content. It has the least energy content among most molecules in the universe. Ramadan [5] reviewed green to green or fully green systems. Hydrogen is produced with special kind of these systems by solar energy. Solar energy converts to electrical energy in the solar panels and then the obtained electrical energy is used to produce hydrogen as an important energy source. The energy is stored without air pollution in this method. Wind, geothermal, and wave energies are other energy sources for green to green systems. The pumped hydroelectric, flywheel and compressed air are the other energy storage for green to green systems. Among these systems, the solar-hydrogen coupling systems are the most important, and hence, the researchers have been working on these systems for decade [6,7]. Presently, this substance is employed in many chemical manufacturing units, and their productions are worked with fossil fuels. Electrochemical water splitting is one of the important and prevalent methods for the generation of hydrogen. In recent years, the alkaline electrolyzer has arrived at progressive economic technology to produce hydrogen.

Abdin et al. [8] proposed an improved one-dimensional mathematical model for an alkaline electrolyzer cell to produce hydrogen. The proposed model can be used for different alkaline electrolyzer cells and provide accurate results compared to the same experimental data sets. David et al. [9] presented various methods for hydrogen production. Then some new ways were proposed considering the economic issues. Finally, some new methods were introduced to improve alkaline electrolysis technology. Zakaria and Kamarudin [10] recommended a new anion exchange membrane electrolyzer. Several polymeric membranes were compared with each other in this study. This study has broadly surveyed the influence of important parameters such as ion exchange capability. Brauns and Turek [11] reviewed alkaline water electrolysis operated with renewable energy sources like solar energy. They reported that alkaline water electrolysis is a widespread technology for hydrogen production. Milani et al. [12] have been conducted both experimental and numerical study on the cogeneration unit of

* Corresponding author.
E-mail address: suvash.saha@uts.edu.au (S.C. Saha).

https://doi.org/10.1016/j.ijft.2021.100126

Available online 16 November 2021

aluminum-water reaction. Hydrogen and aluminum were produced in their study. This unit used aluminum as an energy source from the aluminum recycling plant and the water was used in a closed-loop. Omran et al. [13] proposed a new proton-exchange membrane fuel cell unit by the variable load. The electrical current and voltage of the cell was calculated by MATLAB software. They calculate this in the steady-state of the cell. Hence, the variation was independent of time. The power, current, and voltage for the start were 500 W, 12A, and 12 V respectively.

Bideau et al. [14] proposed some equations to determine relations between different parameters in the two classical alkaline electrolytes (KOH, NaOH). In this study, some parameters as electrical conductivity, heat capacity, viscosity, density, mass, and heat transfer diffusion coefficients were calculated with new proposed relations as a function of electrolyte concentration and temperature. The proposed relations have been compared with available experimental data presented by other researchers and worthy agreement was achieved. The efficiency of an electrolyzer mostly depends on the electrical and thermal resistances and over-potential in the cell [15].

Lim et al. [16] reviewed the performance of anion exchange membrane as a solid electrolyte in electrolyzer uses. The enhancement of anion exchange membrane depends on the physicochemical properties, ion exchange capacity, etc. Also, it depends on the thermo-mechanical steadiness in higher temperatures and pH environments. Lafforgue et al. [17] challenged the typically thought about carbon-supported electro-catalysts and their stability in the alkaline environment. This thought was created due to the higher thermodynamics steadiness of several metals at higher pH. This report proved that their typically thought was wrong in aqueous alkaline electrolytes.

Gómez et al. [18] considered the effect of the dynamic operation on the electrolyzer efficiency. In the previous studies, the models for the electrical field were mostly semi-experimental and experimental relations, and the dynamic operation effect was usually ignored. This research summarized and analyzed the proposed schemes to explain the electrical field. Also, the dynamic operation subject was emphasized, and the latest researches modeled the dynamics approach was presented in this study. Mohammadi and Mehrpooya [19] reviewed the performance of different approaches of connection between electrolyzer systems and different clean and interminable energy sources, including solar energy, ocean thermal energy, wind energy, and hydroelectric energy. This research compared these renewable energy sources based on how these sources can be integrated and which one has the best efficiency. Lastly, these energy sources are compared with each other by the thermos-economical view.

In this research, a commercial alkaline electrolyzer is simulated in different temperatures, pressure, thermal resistance, and the influence of these parameters on alkaline electrolyzer characteristics is surveyed. The alkaline electrolyzer that works with renewable energy sources doesn't have a constant electrical current. Hence, the influence of alternative electrical current such as sinusoidal electrical current on alkaline electrolyzer is obtained in this work. The generated and outlet heat rate determines the cell's steady-state temperature, and these two important parameters are also determined in this work. In other words, the main objective of this study is to survey the performance of an alkaline electrolyzer with non-constant currents in a different range of temperature and pressure.

2. System description and principle of operation

In this research, an alkaline electrolyzer is simulated in different conditions. The characteristics of this alkaline electrolyzer are displayed in Table 1.

Table 1
The characteristics of the simulated alkaline electrolyzer.

Cell pressure	1–120 (bar)	The surface area of the electrode	0.25 (m^2)
Cell temperature	380–430 (K)	Thermal resistance	0.1–6.4 (K/W)
Ambient temperature	300 (K)	specific heat capacity of H_2	14.4 (kJ/kg.K)
Electrical Current	0–400 (A)	specific heat capacity of O_2	0.92 (kJ/kg.K)
Overall thermal capacity	625 (kJ/K)	specific heat capacity of H_2O	4.18 (kJ/kg.K)
KOH concentration	30	Water Latent heat	2420 (kJ/kg.K)
Number of cells	20–25		

3. Mathematical modeling of the alkaline electrolyzer: thermal performance

This section tries to mathematically present the thermal performance and related electrochemical properties of a single alkaline electrolyzer cell according to empirical expressions. Then the final goal is to estimate the instant temperature of the cell regarding the supplied current. To start the model, we state the thermal energy balance of the cell. The amount of energy entered to and generated within the cell is equal to the amount of thermal energy consumed and stored as well:

$$\dot{E}_{in} + \dot{E}_{gen} = \dot{E}_{out} + \dot{E}_{st} \tag{1}$$

As long as the cell generates heat during the electrochemical process and the temperature goes up, stored energy equals the amount of generated thermal energy through passing electrical current to commence the process. At the same time, a specified quantity will dissipate to the ambient due to lower temperature. We assume that ambient temperature is lesser than the operating temperature of the electrolyzer, so no thermal energy is entered into the control volume. So:

$$\dot{E}_{st} = \dot{E}_{gen} - \dot{E}_{out} \tag{2}$$

We can assume a lumped thermal capacitance model [20] to express the amount of stored energy. It considers no temperature gradient within the cell and the spatial distribution of temperature is not meaningful. Then this temperature is a kind of average temperature assigned to the cell. So we can write:

$$\dot{E}_{st} = C_{th}\frac{dT}{dt} \tag{3}$$

where C_{th} and T are the overall thermal capacity and the average temperature of the alkaline electrolyzer, respectively, the value of generated energy directly depends on the properties of the electrochemical process taking place within the cell and supplied current. As discussed in the previous section, an alkaline electrolyzer doesn't generate heat at thermoneutral voltage while real electrolyzers always work above that voltage. So the difference of operating voltage and thermoneutral voltage will show the amount of power generation in the form of heat:

$$\dot{E}_{gen} = \left(V - V_{T,P}^{tn}\right)I \tag{4}$$

where V and $V_{T,P}^{tn}$ are operating voltage and thermoneutral voltage at temperature T and pressure P. I is the current supplied from any source such as an electrical network or any renewable resources. The current has the responsibility of providing required electrons to the electrochemical process at the electrodes to lead to valuable gasses O_2 and H_2. But while producing these gasses, attached bubbles are created reducing the effective area of the electrodes. To account for this phenomenon, we define the coefficient θ affecting the current effective area. Rescaling Eq. (4), it turns into Eq. (5) as follows [21,22].

$$\dot{E}_{gen} = \dot{Q}_{gen} = \left(V - V_{T,P}^{tn}\right)\frac{I}{(1-\theta)} \tag{5}$$

θ varies between 0 and 1. Zero value shows the ideal case without any adhered bubble, whereas in the case of θ=1, very large bubbles are attached to the electrodes, prohibiting the appropriate chemical reaction, and a higher value of heat is dissipated.

The second term in Eq. (2), the amount of dissipated thermal energy, consists of three main terms, including heat loss to the environment, exchanging enthalpies, and cooling effect:

$$\begin{aligned} \dot{E}_{out} &= \dot{Q}_{loss} + \dot{Q}_{exch} + \dot{Q}_{cool} \\ C_{th}\frac{dT}{dt} &= \dot{Q}_{gen} - \dot{Q}_{loss} - \dot{Q}_{exch} - \dot{Q}_{cool} \end{aligned} \tag{6}$$

Heat loss to the ambient has two influencing parameters: temperature difference of the cell and ambient and convective heat transfer regime of exterior surface. So we can express as follow:

$$\dot{Q}_{loss} = \frac{T - T_{amb}}{R_{th}} \tag{7}$$

where R_{th} and T_{amb} are total thermal resistance of convective heat transfer and ambient temperature.

Sensible and latent heats contribute as exchanging enthalpies. Enthalpies attributed to the exiting H_2 and O_2 and reagent water fed into the electrolyte to keep KOH concentration at a constant level are sensible heats. Moreover, the specified amount of water turns into vapor at different saturation temperatures and pressures, called latent heat. So we can write:

$$\dot{Q}_{exch} = \dot{m}_{H_2}C_{p,H_2}(T - T_{amb}) + \dot{m}_{O_2}C_{p,O_2}(T - T_{amb}) + \dot{m}_{H_2O}C_{p,H_2O}(T - T_{amb}) + \dot{m}_{Vapor}\lambda_{H_2O} \tag{8}$$

where $\dot{m}_{H_2}$, $\dot{m}_{O_2}$, $\dot{m}_{H_2O}$ and $\dot{m}_{Vapor}$ are mass flow rate of leaving H_2, O_2, reagent liquid water, and mass flow of evaporated water, respectively. C_{p,H_2}, C_{p,O_2}, C_{p,H_2O} and λ_{H_2O} are specific heat capacity of H_2, O_2, and reagent water and latent heat of vaporization of liquid water at the operating temperature and pressure. Disappeared liquid water turns into gasses and vapor. So we can establish the following mass balance:

$$\dot{m}_{H_2O} = \dot{m}_{H_2} + \dot{m}_{O_2} + \dot{m}_{Vapor} \tag{9}$$

Mass flow of water, O_2, and H_2 can be evaluated conveniently according to Faraday's law:

$$\dot{n}_{O_2} = \frac{I\eta_F}{4F}N_C \tag{10}$$

$$\dot{n}_{H_2} = \frac{I\eta_F}{2F}N_C \tag{11}$$

$$\dot{n}_{H_2O} = \frac{I\eta_F}{2F}N_C \tag{12}$$

where N_c, F and η_F are the number of cells, Faraday's constant, and Faraday efficiency defined as the fraction of the actual hydrogen mass flow rate over the theoretical one (usually above 90%). Electrical current is a known parameter for our problem, and Faraday efficiency can be evaluated as following empirical correlation [23]:

$$\eta_F = \left(\frac{i^2}{f_{11} + f_{12}T + i^2}\right).(f_{21} + f_{22}T) \tag{13}$$

Unidentified constants above equation have been recommended as following [23]:

$$f_{11} = 50, f_{12} = 2.5,\ f_{21} = 1, f_{22} = -2.5 \times 10^{-4} \tag{14}$$

By calculating the mass flow of water, O_2, and H_2, water vapor mass flow is evaluated using Eqs. (10)–(12).

The cooling liquid, usually water, absorbs the heat to prohibit the system from reaching a critical temperature:

$$\dot{Q}_{cool} = \dot{m}_{CW}C_{p,CW}\left(T_{CW,out} - T_{CW,in}\right) = UA_{HX}LMTD \tag{15}$$

$$LMTD = \frac{\left(T - T_{CW,out}\right) - \left(T - T_{CW,in}\right)}{ln\left(\left(T - T_{CW,out}\right)/\left(T - T_{CW,in}\right)\right)} \tag{16}$$

where $\dot{m}_{CW}$, $C_{p,CW}$, $T_{CW,out}$ and $T_{CW,in}$ are the mass flow and the specific heat of cooling water and the outlet and the inlet temperatures of the cooling water respectively. The inlet temperature of cooling water usually equals the ambient temperature. UA_{HX} and $LMTD$ are specified terms in the heat exchanger field of study that express the product of thermal exchange coefficient, and the surface of the equivalent heat exchanger, and the log mean temperature difference of the heat exchanger. Rewriting the Eq. (16), we can express (considering $T_{amb} = T_{CW,in}$):

$$\dot{Q}_{cool} = \dot{m}_{CW}C_{p,CW}\left(1 - exp\left(-\frac{UA_{HX}}{\dot{m}_{CW}C_{p,CW}}\right)\right)(T - T_{amb}) \tag{17}$$

In the following, thermos-neutral and operating voltages are discussed. Thermo-neutral voltage consists of two key parameters: high heating voltage ($V_{T,P}^{HHV}$) at pressure P and temperature T and amount of heating difference value from the reference temperature and reference pressure ($H_{T,P_w}^{w(g)} - H_{T_0,P_0}^{w(l)}$), usually ambient condition (P_0 and T_0) [22]:

$$V_{T,P}^{tn} = V_{T,P}^{HHV} + \frac{\varphi}{nF}\left(H_{T,p_{H_2O,KOH}^{saturation}}^{w(g)} - H_{T_0,P_0}^{w(l)}\right) \tag{18}$$

$$H_{T,P_w}^{w(g)} - H_{T_0,P_0}^{w(l)} = 42,960 + 40.762T - 0.06682T^2 \tag{19}$$

where nF=192973C/mol ($n = 2$ for alkaline electrolyzer electrochemical process) and φ is:

$$\varphi = 1.5\frac{p_{H_2O,KOH}^{saturation}}{P - p_{H_2O,KOH}^{saturation}} \tag{20}$$

$p_{H_2O,KOH}^{saturation}$ is water vapor partial pressure over the electrolyte in each electrode at P and T, and we assume that $P = p_{H_2O,KOH}^{saturation} + p_{H_2} = p_{H_2O,KOH}^{saturation} + p_{O_2}$. High heating value can be obtained as following [22]:

$$V_{T,P}^{HHV} = V_{T,P_0}^{HHV} + f_{HHV}(T,P) \tag{21}$$

where V_{T,P_0}^{HHV} and $f_{HHV}(T,P)$ are high heating value at temperature T and atmospheric pressure and pressure correcting factor, respectively [22]:

$$f_{HHV}(T,\ P(in\,bar)) = \left(21.661 \times 10^{-6} - \frac{10.941 \times 10^{-3}}{T}\right)p + \left(\frac{18.578 \times 10^{-6}}{T} + \frac{0.339 \times 10^{-3}}{T^{1.5}} + \frac{7.845 \times 10^{-3}}{T^2} - \frac{1.659}{T^3}\right)p^2 \tag{22}$$

$$V_{T,P_0}^{HHV} = 1.4756 + 2.252 \times 10^{-4}T + 1.52 \times 10^{-8}T^2 \tag{23}$$

To evaluate saturation pressure of steam over KOH, the following relations are applicable [24]:

$$p_{H_2O,KOH}^{saturation} = exp\left(2.302a + bln\, p_{Pure-H_2O}^{saturation}\right)\ (in\ bar)$$
$$a = -0.0151m - 1.6788\times10^{-3}m^2 + 2.2588\times10^{-5}m^3 \quad (24)$$
$$b = 1 - 1.2062\times10^{-3}m + 5.6024\times10^{-4}m^2 - 7.8228\times10^{-6}m^3$$

$$p_{Pure-H_2O}^{saturation} = exp\left(81.6179 - \frac{7699.68}{T} - 10.9lnT + 9.5891\times10^{-3}T\right)(in\ bar) \quad (25)$$

Where a and b are coefficients related to the KOH concentration, and $p_{Pure-H_2O}^{saturation}$ is steam saturation pressure over pure water. These recommended experimental equations can be applied for temperatures between 0 °C and 250 °C, pressures between 1 and 200 kPa, and molar concentration range between 2 and 18 mol/Kg.

To calculate the working value of cell voltage, over-potentials at the cell should be comprehensively calculated and added to the reversible voltage while representing them in mathematical equations. Therefore, the cell voltage is the sum of reversible voltage and over potentials [8]:

$$V = V_{oc} + V_{act} + V_{ohm} \quad (26)$$

where V_{OC}, V_{act} and V_{ohm} are the amount of open-circuit voltage or reversible voltage, activation overpotential, and ohmic overpotential, respectively. The reversible voltage is obtained according to the Nernst equation as follows [8,25,26]:

$$V_{OC} = V_{P_0,T}^{rev} + \frac{R^*T}{2F}\left(ln\left(\frac{pH_2\sqrt{po_2}}{\alpha_{H_2}o,KOH}\right)\right) = V_{p_0,T}^{rev} + \frac{R^*T}{2F}ln\left(\frac{\left(p - p_{H_0O,KOH}^{saturation}\right)^{3/2}}{\alpha_{H_2}o,KOH}\right) \quad (27)$$

$$V_{P_0,T}^{rev} = 1.5184 - 1.5421\times10^{-3}\times T + 9.526\times10^{-5}\times T\times lnT + 9.84\times10^{-8}\times T^2 \quad (28)$$

where $V_{P_0,T}^{rev}$ and $\alpha_{H_2O,KOH}$ are reversible voltage at standard conditions. But, there are some limitations in using this relation even for those dilute solutions or higher concentrations and even when there is net current flow through the electrodes; because of the action of ions variations at the surface of electrodes [26]. And the water activity of the KOH solution is obtained [27]:

$$\alpha_{H_2O,KOH} = exp\left(-0.05192m + 0.003302m^2 + \frac{(3.177m - 2.131m^2)}{T}\right) \quad (29)$$

which is acceptable for temperatures between 0 °C and 250 °C, pressures between 1 and 200 kPa, and molar concentration range between 2 and 18 mol/Kg.

To calculate the activation over-potential, we use the Butler-Volmer relation for both electrodes according to the transition state theory [28,29]. Hence, one has:

$$V_{act}^{anode} = \frac{R^*T}{\alpha_{anode}F}\left[ln\left(\frac{i}{i_0^{anode}}\right)\right] \quad (30)$$

$$V_{act}^{cathode} = \frac{R^*T}{\alpha_{cathode}F}\left[ln\left(\frac{i}{i_0^{cathode}}\right)\right] \quad (31)$$

where i_0 is the effective exchange current density (I/A_e) of the electrode and is forecast at any temperature supposing activated mechanism [11,12]:

$$i_0 = \gamma_M \times exp\left[-\frac{\Delta G_C}{R^*}\left(\frac{1}{T} - \frac{1}{T_{ref}}\right)\right]i_{0,ref} \quad (32)$$

where γ_M, ΔG_C, T_{ref} and $i_{0,ref}$ are roughness factor, the free energy of activation, reference temperature, and reference exchange current density at T_{ref}, respectively. To contribute the covered portion of the electrode with bubbles, activation over-potential is rewritten as follow [8]:

$$V_{act}^{anode} = \frac{R^*T}{\alpha_{anode}F}\left[ln\left(\frac{i}{i_0^{anode}(1-\theta_{anode})}\right)\right] \quad (33)$$

$$V_{act}^{cathode} = \frac{R^*T}{\alpha_{cathode}F}\left[ln\left(\frac{i}{i_0^{cathode}((1-\theta_{cathode}))}\right)\right] \quad (34)$$

Estimation bubble coverage factor (θ) is important, and it has numerous parameters such as natural or forced circulation of aqueous, surface tension of the liquid, and so on those affect the bubble coverage factor. Hence, an experimental relation is used to calculate the bubble coverage factor [22–24,30].

$$\theta = \left[-97.25 + 182\frac{T}{T_{ref}} - 84\left(\frac{T}{T_{ref}}\right)^2\right]\times\left(\frac{i}{i_{lim}}\right)^{0.3}\times\frac{P}{P - p_{H_2O,KOH}^{saturation}} \quad (35)$$

Here i_{lim} is the restrictive current density at 100% bubble coverage with a usual value of 300 kAm^{-2} [21,31]. Ohmic over-potential is a function of electrical current and is the sum of three main ohmic resistances: these three main ohmic resistances are electrolyte resistance, electrodes resistance, and separator resistance. [8]:

$$R_{electrode} = R_{anode} + R_{cathode} = \frac{\rho_o^{anode}}{(1-\varepsilon_{anode})^{3/2}}\frac{\delta_{anode}}{A_e}\left[1 + K_{anode}\left(T - T_{ref}\right)\right] + \frac{\delta_{cathode}}{A_e}\left[1 + K_{cathode}\left(T - T_{ref}\right)\right] \quad (36)$$

where ρ_0, ε, δ, κ and A_e are the resistivity of the one hundred percent dense anode/cathode material at the ambient temperature, porosity, thickness, temperature coefficient of resistivity, and external electrode surface area, respectively. To calculate electrolyte resistance, it should be calculated into two parts. The first part is bubble zone and the second one is bubble free-zone for each terminal, and according to fundamental electrical resistance and Bruggeman's relation, one has [8,32,33]:

$$R_{electrolyte} = R_{electrolyet}^{anode} + R_{electrolyte}^{cathode} = \frac{\rho_{electrolyet,\,ref}}{\left[1 + K_{electrolyte}\left(T - T_{ref}\right)\right]}\times\left[\frac{l_{anode-s} - \beta_{anode}}{A_e} + \frac{1}{(1-\theta_{anode})^{3/2}}\frac{\beta_{anode}}{A_e} + \frac{l_{cathode-s} - \beta_{cathode}}{A_e} + \frac{1}{(1-\theta_{cathode})^{3/2}}\frac{\beta_{cathode}}{A_e}\right] \quad (37)$$

where $\rho_{electrolyte,ref}$, $l_{anode-s}$ or $l_{cathode-s}$ and β are effective resistivity of electrolytes at the ambient temperature, bubble-free zone width, and bubble zone width, respectively. The resistance of the separator is calculated by [8,34,35]:

$$R_{seperator} = \rho_{electrolyte} \frac{\tau^2_{seperator} \delta_{seperator}}{\omega_{seperator} \times \varepsilon_{seperator} \times A_{seperator}} \quad (38)$$

where τ, ω, A and ε are tortuosity, wettability factors for electrolyte, uniform distribution cross-section, and porosity, respectively. The total resistance is calculated by

$$R_{total} = R_{electrode} + R_{electrolyte} + R_{seperator} \quad (39)$$

where $R_{total}, R_{electrode}, R_{electrolyte}, and R_{seperator}$ are total, electrode, electrolyte, and separator resistances, respectively. The ohmic overpotential is obtained by

$$V_{ohm} = Ri \quad (40)$$

where $V_{ohm}$is ohmic over potential "R" is total resistance, and "i" is the electrical current.

4. Results and discussion

The proposed system has been simulated in different conditions and the results of simulations have been displayed in this section. The main limitation of the proposed model is its electrical current. This system is proposed to work with solar energy and therefore, the input electrical current is the main limitation of this system. The temperature of the alkaline electrolyzer is considered constant in different space and it varies with time. In other words, the mean temperature at each time is used as the temperature of the proposed system. For future works, the temperature field of the proposed system can be found by one of the computational fluid dynamics methods [36] for more accuracy.

Thermoneutral voltage versus pressure at different temperatures is obtained and compared with the results of Hammoudi et al. [22] for validation in Fig. 1. Good agreement is observed. The results show that the thermoneutral voltage decreases when pressure increases for small pressure and is constant for large pressures. Also, the results show that the thermoneutral voltage increases by temperature increasing. Another validation is done with the results of Hug et al. [37]. The Faraday efficiency versus electrical current at different temperatures is calculated and compared with the results of Hug et al. [37] in Fig. 2. This figure

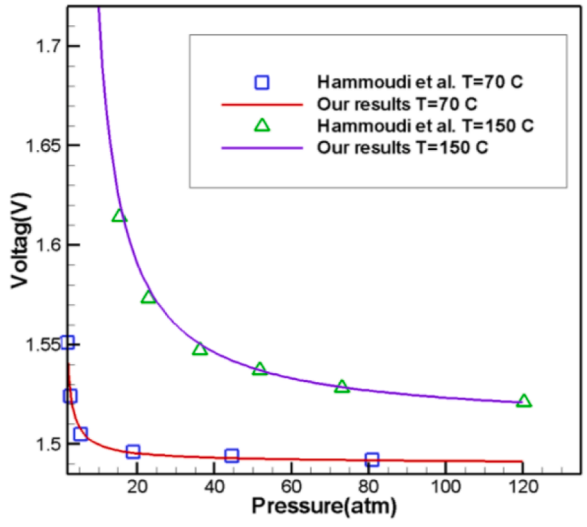

Fig. 1. Thermoneutral voltage versus pressure at different temperatures (present work and Hammoudi et al. results) [22].

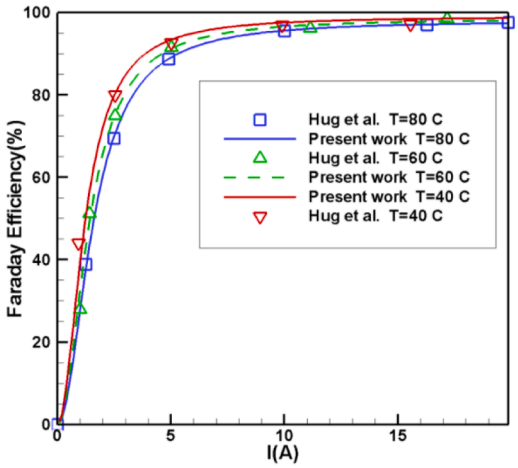

Fig. 2. Comparison between the results of present work and Hug et al. [37]. (Faraday efficiency).

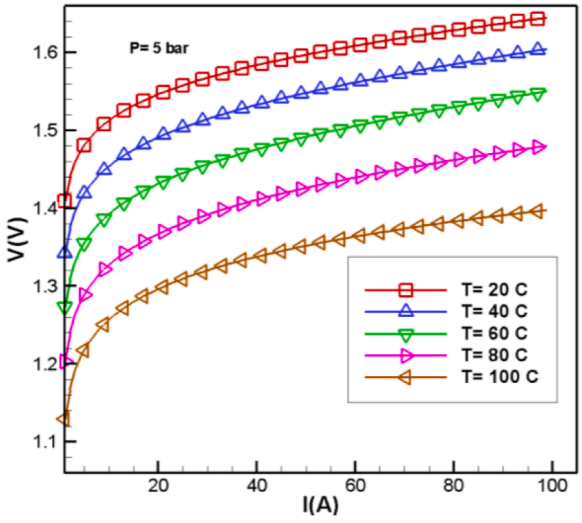

Fig. 3. The cell voltage variation versus electrical current at different temperatures.

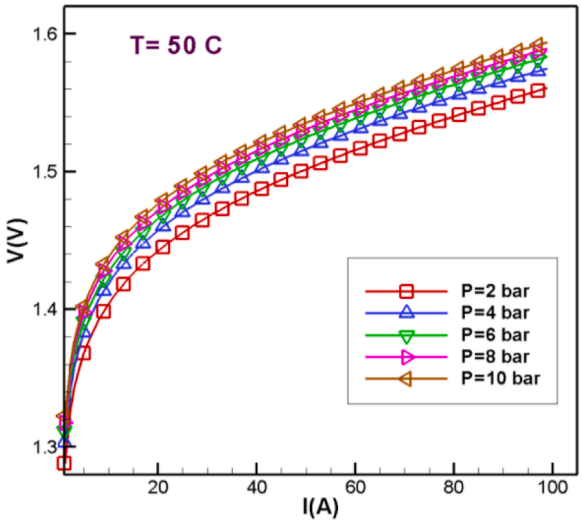

Fig. 4. Cell voltage variation versus electrical current at different pressures.

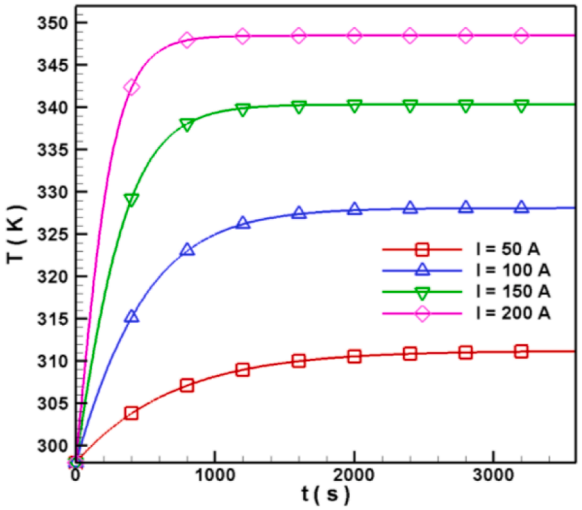

Fig. 5. Temperature variation versus time at different electrical currents.

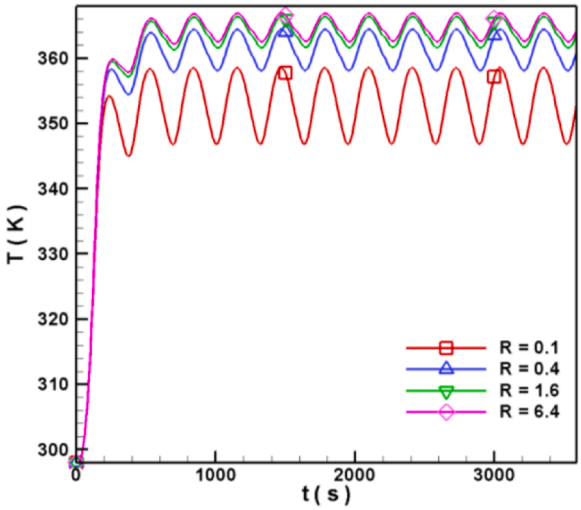

Fig. 7. Temperature variation versus time at different thermal resistances of the cell (sinusoid electrical current).

confirms the accuracy of the current model.

The cell voltage variation versus electrical current at different temperatures is shown in Fig. 3. The cell voltage increases by electrical current increasing and temperature decreasing. The cell voltage variation decreases at high electrical currents. The cell voltage variation versus electrical current at different pressure is shown in Fig. 4. According to Fig. 4, the Cell voltage rises by electrical current increasing when pressure increases, but results show that the cell voltage variation by pressure is negligible.

When an Alkaline Electrolyser works, the temperature of fluid changes with time. Hence, an Alkaline Electrolyser has an unsteady process. Temperature variation versus time at different constant electrical currents is calculated according to the mentioned relations in Section 3 and is shown in Fig. 5. A nonlinear first-order ordinary differential equation should be solved to obtain the temperature variation at different times. This nonlinear equation has been solved by an especial fifth-order Runge-Kutta method numerically [38,39]. The applied numerical method has high accuracy and it uses memory less than the ordinary Runge-Kutta method [40].

The temperature of the Alkaline Electrolyser rises faster in high electrical currents. When the temperature of the Alkaline Electrolyser rises, the cell voltage decreases, and the Thermoneutral voltage increases. Hence, the differences between the cell voltage decreases and the Thermoneutral voltage decreases. The produced heat rate inside the Alkaline Electrolyser depends on the differences between the cell voltage decreases and the Thermoneutral voltage. As a result, raising the temperature of the Alkaline Electrolyser reduces the produced heat rate. Also, increasing the temperature of the Alkaline Electrolyser increases the temperature difference between the inside and the outside of the Alkaline Electrolyser. As a result, the outlet(deposed) heat rate increases. Decreasing the produced heat rate and increasing the outlet heat rate slows down the growth of the temperature of Alkaline Electrolyser, and finally, the temperature of the container reaches the equilibrium temperature.

Electric current is not always constant. For example, it can be sinusoidal. The electrical current produced by solar energy is not constant. In this section, to investigate the effect of these currents on the characteristics of the Alkaline Electrolyzer, the current is assumed to be sinusoidal. The results are shown in Figs. 6 and 7. The cell voltage variation versus time at different sinusoid electrical currents is shown in Fig. 6. As observed, the Alkaline Electrolyser's temperature rises to an especial amount, and then it changes sinusoidally. In other words, there isn't any final equilibrium temperature in this state, but the average temperature

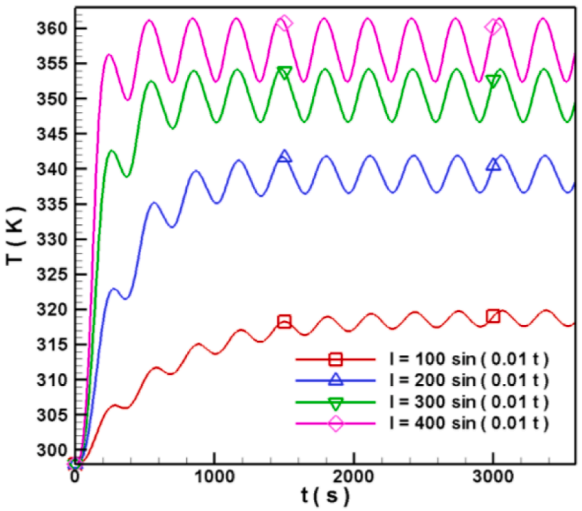

Fig. 6. Cell voltage variation versus time at different sinusoid electrical current.

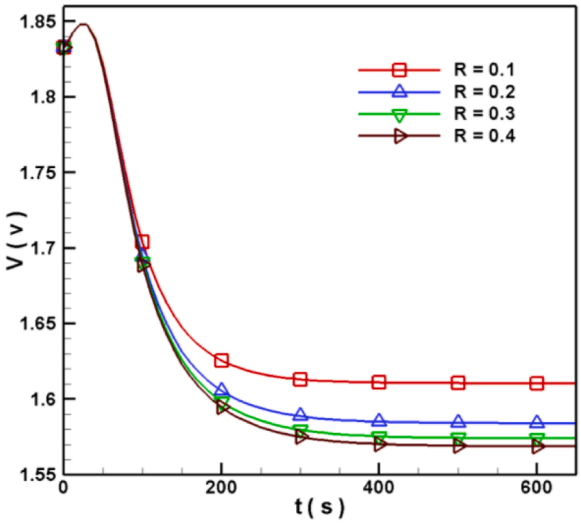

Fig. 8. Voltage variation versus time at different thermal resistances of the cell (constant current).

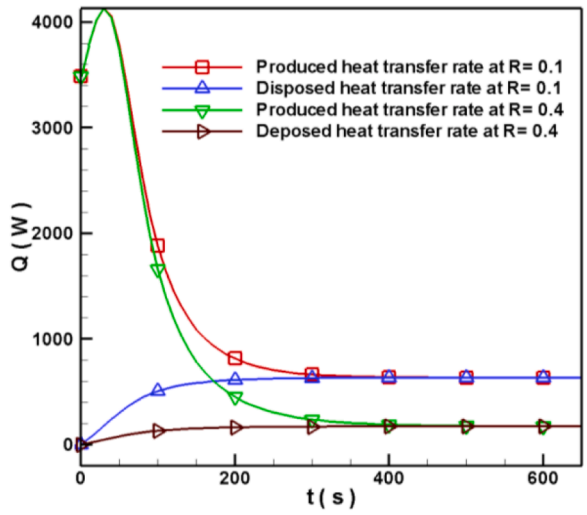

Fig. 9. Produced and disposed heat rate versus time at different thermal resistance of the cells and constant current.

remains constant after a while. The thermal resistance of walls in an electrolyzer is a function of their material and thickness. In this section, the influence of this thermal resistance on the electrolyzer performance is surveyed. Temperature variation versus time at different thermal resistances of the cell for sinusoidal electrical current is calculated and displayed in Fig. 7.

As thermal resistance increases, the outlet heat rate decreases. As a result, the equilibrium temperature becomes higher than before. Increasing the equilibrium temperature decreases the cell voltage and increases the Thermoneutral voltage, thus reducing the voltage difference. Reducing the voltage difference reduces the generated heat. Also, increasing the equilibrium temperature increases the outlet heat rate. Hence, the electrolyzer reaches the new equilibrium temperature faster. As a result, with a further increase in the thermal resistance of the electrolyzer, there is not much change in the equilibrium temperature. The cell Voltage variation versus time at different thermal resistances of the cell is obtained and shown in Fig. 8. The cell voltage decreases over time due to the increase in the temperature of the electrolyzer and eventually reaches a certain value because the temperature of the electrolyzer has reached the equilibrium temperature. As the electrolyzer's thermal resistance increases, the cell voltage's final value is lower due to the lower equilibrium temperature of the electrolyzer. Due to the mentioned reasons in the previous sections, with a further reduction of thermal resistance, the reduction of the final voltage is negligible.

The generated and outlet heat rates are obtained and displayed in Fig. 9. The generated heat rate decreases over time. The generated heat increases the temperature of the electrolyzer. Increasing the temperature of the electrolyzer decreases the generated heat rate and increases the outlet heat rate. As a result, the generated heat rate decreases, and the outlet heat rate increases until they become equal and the electrolyzer reaches the steady-state conditions. The steady-state conditions happen at high heat generated rate at low thermal resistance.

5. Conclusion

In this study, commercial alkaline electrolyzers have been simulated. Different condition as different pressure, electrical current, thermal resistance have been considered for the simulations. The pressure and the temperature in the simulations are between 1 and 100 bar and between 300 and 360 Kelvin respectively. The obtained results show that the thermoneutral voltage decreases when pressure increases. Also, the thermoneutral voltage is high in high cell temperatures. The Faraday efficiency increases when electrical current increases and its variation by temperature and pressure is negligible. The cell voltage increases by the electrical current increasing. It is low in high cell temperatures and changes with pressure variation slightly. When an alkaline electrolyzer starts to work, the generated heat increases cell temperature. Increasing cell temperature decreases generated heat rate and increases outlet heat rate. As a result, an increase in the cell temperature becomes slowly, and finally, the alkaline electrolyzer reaches the steady-state condition and temperature. Sinusoidal electoral current is applied in the alkaline electrolyzer to see the influence of inconstant current on alkaline electrolyzer characteristics. Results show that the alkaline electrolyzer does not reach steady-state conditions in sinusoidal electrical current. The results show that the equilibrium temperature is reached 2–3 h after the time that the Alkaline electrolyzer starts to work. The results also show that the equilibrium temperature depends on the characteristics of the alkaline electrolyzer like thermal resistance, electrical current, and pressure. The equilibrium temperature is between 309 and 368 Kelvin for the simulated systems according to the results. The efficiency of an alkaline electrolyzer depends on temperature strongly. As a result, the mean temperature of the alkaline electrolyzer should be limited.

Declaration of Competing Interest

None

References

[1] A. Sharif, M.S. Meo, M.A.F. Chowdhury, K. Sohag, Role of solar energy in reducing ecological footprints: an empirical analysis, J. Clean. Prod. 292 (2020), 126028, https://doi.org/10.1016/j.jclepro.2021.126028, 2021/04/10/2021, doi: https://doi.org/.

[2] T. Adibi, Evaluation of using solar ammonia absorption cooling system for major cities of the Middle East, Int. J. Heat Technol. 36 (3) (2018) 840–846, https://doi.org/10.18280/ijht.360309.

[3] T.R. Ayodele, A.A. Yusuff, T.C. Mosetlhe, M. Ntombela, Hydrogen production using solar energy resources for the South African transport sector, Int. J. Sustain. Eng. (2021) 1–15, https://doi.org/10.1080/19397038.2021.1970276.

[4] S.A. Haider, M. Sajid, S. Iqbal, Forecasting hydrogen production potential in islamabad from solar energy using water electrolysis, Int J Hydrogen Energy 46 (2) (2020) 1671–1681, https://doi.org/10.1016/j.ijhydene.2020.10.059, 2021/01/06/2021, doi: https://doi.org/.

[5] M. Ramadan, A review on coupling Green sources to Green storage (G2G): case study on solar-hydrogen coupling, Int. J. Hydrogen Energy 46 (59) (2020) 30547–30558, https://doi.org/10.1016/j.ijhydene.2020.12.165, 2021/08/26/2021, doi: https://doi.org/.

[6] F.I. Gallardo, A. Monforti Ferrario, M. Lamagna, E. Bocci, D. Astiaso Garcia, T. E. Baeza-Jeria, A techno-economic analysis of solar hydrogen production by electrolysis in the north of Chile and the case of exportation from Atacama Desert to Japan, Int. J. Hydrogen Energy 46 (26) (2020) 13709–13728, https://doi.org/10.1016/j.ijhydene.2020.07.050, 2021/04/14/2021, doihttps://doi.org/.

[7] N. Khelfaoui, A. Djafour, C. Ghenai, I. Laib, M.B. Danoune, A. Gougui, Experimental investigation of solar hydrogen production PV/PEM electrolyser performance in the Algerian Sahara regions, Int. J. Hydrogen Energy 46 (59) (2020) 30524–30538, https://doi.org/10.1016/j.ijhydene.2020.11.193, 2021/08/26/2021, doi: https://doi.org/.

[8] Z. Abdin, C.J. Webb, E.M. Gray, Modelling and simulation of an alkaline electrolyser cell, Energy 138 (2020) 316–331, https://doi.org/10.1016/j.energy.2017.07.053, 2017/11/01/2017, doi: https://doi.org/.

[9] M. David, C. Ocampo-Martínez, R. Sánchez-Peña, Advances in alkaline water electrolyzers: a review, J. Energy Storage 23 (2020) 392–403, https://doi.org/10.1016/j.est.2019.03.001, 2019/06/01/2019, doi: https://doi.org/.

[10] Z. Zakaria, S.K. Kamarudin, A review of alkaline solid polymer membrane in the application of AEM electrolyzer: materials and characterization, Int. J. Energy Res. (2020) https://doi.org/10.1002/er.6983vol. n/a, no. n/a, 2021/06/24 2021, doi: https://doi.org/10.1002/er.6983.

[11] J. Brauns, T. Turek, Alkaline water electrolysis powered by renewable energy: a review, Processes 8 (2) (2020) 248 [Online]. Available: https://www.mdpi.com/2227-9717/8/2/248.

[12] M. Milani, Experimental and numerical analysis of a liquid aluminium injector for an Al-H2O based hydrogen production system, Int. J. Thermofluids (2020), https://doi.org/10.1016/j.ijft.2020.100018 vol. 7-8, p. 100018, 2020/11/01/2020, doi: https://doi.org/.

[13] A. Omran, Mathematical model of a proton-exchange membrane (PEM) fuel cell, Int. J. Thermofluids 11 (2020), 100110, https://doi.org/10.1016/j.ijft.2021.100110, 2021/08/01/2021, doi: https://doi.org/.

[14] D.Le Bideau, P. Mandin, M. Benbouzid, M. Kim, M. Sellier, Review of necessary thermophysical properties and their sensivities with temperature and electrolyte mass fractions for alkaline water electrolysis multiphysics modelling, Int. J.

Hydrogen Energy 44 (10) (2020) 4553–4569, 2019/02/22/2019, doi: https://doi.org/10.1016/j.ijhydene.2018.12.222.
[15] A.L. Santos, M.-J. Cebola, D.M.F. Santos, Towards the hydrogen economy—a review of the parameters that influence the efficiency of alkaline water electrolyzers, Energies 14 (11) (2021), https://doi.org/10.3390/en14113193 doi:.
[16] K.L. Lim, Radiation-grafted anion-exchange membrane for fuel cell and electrolyzer applications: a mini review, Membranes 11 (6) (2021), https://doi.org/10.3390/membranes11060397.
[17] C. Lafforgue, A. Zadick, L. Dubau, F. Maillard, M. Chatenet, Selected review of the degradation of Pt and Pd-based carbon-supported electrocatalysts for alkaline fuel cells: towards mechanisms of degradation, Fuel Cells 18 (3) (2020) 229–238, https://doi.org/10.1002/fuce.201700094, https://doi.org/10.1002/fuce.2017000942018/06/01 2018, doi: https://doi.org/.
[18] Á. Hernández-Gómez, V. Ramirez, D. Guilbert, Investigation of PEM electrolyzer modeling: electrical domain, efficiency, and specific energy consumption, Int. J. Hydrogen Energy 45 (29) (2020) 14625–14639, 2020/05/26/2020, doi: https://doi.org/10.1016/j.ijhydene.2020.03.195.
[19] A. Mohammadi, M. Mehrpooya, A comprehensive review on coupling different types of electrolyzer to renewable energy sources, Energy 158 (2018) 632–655, https://doi.org/10.1016/j.energy.2018.06.073. /09/01/2018, doi: https://doi.org/.
[20] F.P.I. Theodore, L. Bergman, D.P. DeWitt, A.S. Lavine, Fundamentals of Heat and Mass Transfer, John Wiley & Sons, 2011.
[21] H. Vogt, R.J. Balzer, The bubble coverage of gas-evolving electrodes in stagnant electrolytes, Electrochim. Acta 50 (10) (2005) 2073–2079, https://doi.org/10.1016/j.electacta.2004.09.025. /03/15/2005, doi: https://doi.org/.
[22] M. Hammoudi, C. Henao, K. Agbossou, Y. Dubé, M.L. Doumbia, New multi-physics approach for modelling and design of alkaline electrolyzers, Int. J. Hydrogen Energy 37 (19) (2012) 13895–13913, https://doi.org/10.1016/j.ijhydene.2012.07.015. /10/01/2012, doi: https://doi.org/.
[23] Ø. Ulleberg, Modeling of advanced alkaline electrolyzers: a system simulation approach, Int. J. Hydrogen Energy 28 (1) (2003) 21–33, https://doi.org/10.1016/S0360-3199(02)00033-2. /01/01/2003, doi: https://doi.org/.
[24] J. Balej, Water vapour partial pressures and water activities in potassium and sodium hydroxide solutions over wide concentration and temperature ranges, Int. J. Hydrogen Energy 10 (4) (1985) 233–243, https://doi.org/10.1016/0360-3199(85)90093-X. /01/01/1985, doi: https://doi.org/.
[25] J.C. Amphlett, R.M. Baumert, R.F. Mann, B.A. Peppley, P.R. Roberge, T.J. Harris, Performance modeling of the ballard mark IV solid polymer electrolyte fuel cell: i . mechanistic model development, J. Electrochem. Soc. 142 (1) (1995) 1–8, https://doi.org/10.1149/1.2043866. /01/01 1995, doi:.
[26] J.D.A. Larminie, Fuel Cell Systems Explained, Oxford Brookes University, 2003.
[27] C. Henao, K. Agbossou, M. Hammoudi, Y. Dubé, A. Cardenas, Simulation tool based on a physics model and an electrical analogy for an alkaline electrolyser, J. Power Sources 250 (2014) 58–67, https://doi.org/10.1016/j.jpowsour.2013.10.086. /03/15/2014, doi: https://doi.org/.
[28] T. Thampan, S. Malhotra, J. Zhang, R. Datta, PEM fuel cell as a membrane reactor, Catal. Today 67 (1) (2001) 15–32, https://doi.org/10.1016/S0920-5861(01)00278-4. /05/15/2001, doi: https://doi.org/.
[29] D. Lewis, S. Glasstone, Elements of Physical Chemistry, Macmillan, 1960.
[30] J. Turner, Renewable hydrogen production, Int. J. Energy Res. 32 (5) (2008) 379–407, https://doi.org/10.1002/er.1372, https://doi.org/10.1002/er.1372vol2008/04/01doi: https://doi.org/.
[31] C. Bianchini, PierluigiBarbaro, Catalysis For Sustainable Energy Production, eds., Wiley-Vch, 2009.
[32] A. Perron, L. Kiss, S. Poncsák, Mathematical model to evaluate the ohmic resistance caused by the presence of a large number of bubbles in Hall-Héroult cells, J. Appl. Electrochem. 37 (2007) 303–310.
[33] F. Hine, K. Murakami, Bubble effects on the solution IR drop in a vertical electrolyzer under free and forced convection, J. Electrochem. Soc. 127 (1980) 292–297.
[34] P.H. Vermeiren, R. Leysen, H. Beckers, J.P. Moreels, A. Claes, The influence of manufacturing parameters on the properties of macroporous Zirfon® separators, J. Porous Mater. 15 (3) (2008) 259–264, https://doi.org/10.1007/s10934-006-9084-0, 2008/06/01.
[35] R.J. Gilliam, J.W. Graydon, D.W. Kirk, S.J. Thorpe, A review of specific conductivities of potassium hydroxide solutions for various concentrations and temperatures, Int. J. Hydrogen Energy 32 (3) (2007) 359–364, https://doi.org/10.1016/j.ijhydene.2006.10.062, 2007/03/01/https://doi.org/.
[36] T. Adibi, S.E. Razavi, O. Adibi, M. Vajdi, F. Sadegh Moghanlou, The response of nano-ceramic doped fluids in heat convection models: a characteristics-based numerical approach (in en), Sci. Iran. (2021), https://doi.org/10.24200/sci.2021.56574.4794.
[37] W. Hug, J. Divisek, J. Mergel, W. Seeger, H. Steeb, Highly efficient advanced alkaline electrolyzer for solar operation, Int. J. Hydrogen Energy 17 (9) (1992) 699–705, https://doi.org/10.1016/0360-3199(92)90090-J. /09/01/1992, doi: https://doi.org/.
[38] T. Adibi, O. Adibi, S.E. Razavi, A characteristic-based solution of forced and free convection in closed domains with emphasis on various fluids (in en), Int. J. Eng. 32 (11) (2019) 1689–1695, https://doi.org/10.5829/ije.2019.32.11b.20. doi:.
[39] T. Adibi, S.E. Razavi, O. Adibi, A characteristic-based numerical simulation of water-titanium dioxide nano-fluid in closed domains (in en), Int. J. Eng. 33 (1) (2020) 158–163, https://doi.org/10.5829/ije.2020.33.01a.18.
[40] T. Adibi, Three-dimensional characteristic approach for incompressible thermo-flows and influence of artificial compressibility parameter (in en), J. Comput. Appl. Res. Mech. Eng. 8 (2) (2019) 223–234, https://doi.org/10.22061/jcarme.2018.2032.1178, 02/01doi:.